Silicon accumulation controls carbon cycle in wetlands through modifying nutrients stoichiometry and lignin synthesis of Phragmites australis

Author

Xia, Shaopan, Song, Zhaoliang, Van Zwieten, Lukas, Guo, Laodong, Yu, Changxun, Hartley, Iain P, Wang, Hailong

Published

2020

Journal Title

Environmental and Experimental Botany

Version

Accepted Manuscript (AM)

DOI

10.1016/j.envexpbot.2020.104058

Silicon accumulation controls carbon cycle in wetlands through modifying nutrients stoichiometry and lignin synthesis of *Phragmites australis*

Shaopan Xia[1], Zhaoliang Song[1]*, Lukas Van Zwieten[2], Laodong Guo[3], Changxun Yu[4], Iain P. Hartley[5], Hailong Wang[6,7]

[1] Institute of Surface-Earth System Science, Tianjin University, Tianjin 300072, China

[2] Wollongbar Primary Industries Institute, NSW Department of Primary Industries, Australia

[3] School of Freshwater Sciences, University of Wisconsin-Milwaukee, Wisconsin, America

[4] Department of Biology and Environmental Science, Linnaeus University, Kalmar 39182, Sweden

[5] Geography, College of Life and Environmental Science, University of Exeter, Exeter EX4 4QJ, UK

[6] School of Environment and Chemical Engineering, Foshan University, Foshan, Guangdong 528000, China

[7] School of Environmental and Resource Sciences, Zhejiang A&F University, Hangzhou, Zhejiang 311300, China

*Correspondence to: zhaoliang.song@tju.edu.cn or songzhaoliang78@163.com

Telephone: +086-15202264081

Address: Institute of the Surface-Earth System Science, Tianjin University, Tianjin 300072, China

Abstract

Silicon (Si) is one of the most abundant elements in the Earth's crust but its role in governing the biogeochemical cycling of other elements remains poor understood. There is a paucity of information on the role of Si in wetland plants, and how this may alter wetland C production and storage. Therefore, this study investigated Si distribution, nutrient stoichiometry and lignin abundance in *Phragmites australis* from a wetland system in China to better understand the biogeochemical cycling and C storage. Our data show that Si content (ranging between 0.202% to 6.614%) of *Phragmites australis* is negatively correlated with C concentration (38.150%–47.220%). Furthermore, Si content was negatively antagonistically related to the concentration of lignin-derived phenols in the stem (66.763–120.670 mg g^{-1} C) and sheath (65.400–114.118 mg g^{-1} C), but only a weak relationship was observed in the leaf tissue (36.439–55.905 mg g^{-1} C), which is relevant to the photosynthesis or stabilization function of the plant tissues. These results support the notion that biogenic Si (BSi) can substitute lignin as a structural component, due to their similar eco-physiological functions, reduces costs associated with lignin biosynthesis. The accumulation of BSi increased total biomass C storage and nutrient accumulation due to greater productivity of *Phragmites australis*. On the other hand, BSi regulated litter composition and quality (e.g., nutrient stoichiometry and lignin) that provide a possibility for the factors affecting litter decomposition. Thus competing processes (i.e., biomass quantity vs quality) can be influenced by Si cycling in wetlands.

Keywords: 'Blue Carbon', biogenic silica, lignin, *Phragmites australis*, litter composition and quality, wetland

1 Introduction

Wetlands cover 5–8% of the Earth's land surface, storing around 535 Gt of "blue carbon (C)", representing about 30% of global terrestrial C pool (Mitsch et al., 2013; Krauss et al., 2018; Rogers et al., 2019). "Blue carbon" covers carbon sinks in many habitats such as coastal zones, wetlands, swamps, estuaries, off-shore, shallow and deep oceans, more recently, on the carbon held submarine ecosystems (such as seagrass) and coastal wetland ecosystems (such as mangroves and salt marshes) (Atwood et al., 2015; Nahlik and Fennessy, 2016). *Phragmites australis* is one of the most dominant and successfully established plant species in inland water, riparian wetlands and tidal marshes, typically forming mono-specific stands (Saltonstall, 2002). *Phragmites australis* is a major contributor to organic matter deposition within the wetland systems driving biogeochemical cycling and contributing to ecosystem sustainability (Soetaert et al., 2004; González-Alcaraz et al., 2012).

As the second most abundant element in the earth's crust, silicon (Si) is a beneficial element for plant growth, especially for grasses, ferns, and horsetails (Katz, 2019). Biogenic silicon (BSi) has been shown to be important in mitigating the impacts of many abiotic and biotic stresses to plants. These include pathogen resistance (Wang et al., 2017), drought resistance (Ahmed et al., 2016), salt stress (Bosnic et al., 2018), pest resistance (Laing et al., 2006), and heavy metal tolerance (Imtiaz et al., 2016). *Phragmites australis* is efficient in taking up silica, and storing a large reservoir in the BSi pool (as amorphous silica deposits or phytoliths) (Hou et al., 2010; Li et al., 2013a), and can grow on highly diverse substrates resulting in different silicon availability (Engloner, 2009). The plant is also responsible for releasing Si into the wetland environment

(Struyf et al., 2007), thus playing a crucial role in the biogeochemical cycling of Si in wetlands (Struyf and Conley, 2009; Liang et al., 2015).

The decay of plant litter is controlled in part by the composition of the C compounds (e.g., lignin, cellulose, and phenol) and the elemental stoichiometry of biomass (C: N: P: S) (Fioretto et al., 2005; Hätenschwiler and Jorgensen, 2010; Sun et al., 2018). The Si availability within the plants can influence litter decomposition by affecting litter surface chemistry, including the nutrient content and nutrient stoichiometry, and the nature of the carbon compounds (Schaller and Struyf, 2013; Marxen et al., 2016). To date, studies on plant ecological stoichiometry have focused primarily on C, N and P (Struyf and Conley, 2009; Venterink and Güewell, 2010; Zechmeister-Boltenstern et al., 2015). On the other hand, Si, may exert direct and indirect effects regulating litter composition and quality that provide a possibility for the factors affecting litter decomposition, has received only scant attention in this context. No comprehensive studies on the synergistic effect between Si and other biogenic elements and C cycling in wetlands were found.

The components of organic macromolecules in plant litter, especially cellulose, hemicellulose and lignin, are intrinsic factors in plant litter decomposition (Castellano et al., 2015; García-Palacios et al., 2016). Some studies have shown a subtle connection between the BSi concentration and plant litter decomposition, potentially by influencing litter lignin concentrations (e.g., Talbot and Treseder, 2012; Yue et al., 2016; Ruhland et al., 2018; He et al., 2019). As a major component in plant-derived soil organic carbon (SOC), lignin phenols are considered an important part of the stable soil C pool, which has attracted much attention in the study of SOC preservation and dynamics (Thevenot et al., 2010; Zhu et al., 2019). There is,

however, a paucity of information on the mechanisms by which BSi regulates plant nutrient contents and structural C components within wetland macrophytes, and thus decomposition rates and biogeochemical cycling within wetlands.

The effect of Si-mediated nutrient acquisitions and biomass regulation in wetland systems, as well as lignin synthesis under natural field conditions is largely unknown. As 'blue C' is a globally important store of C (Nahlik and Fennessy, 2016), it is crucial to gain a better understanding of the role of BSi accumulation in regulating plant biomass C accumulation and C emissions by litter decomposition in wetlands. The main objective of this study is to elucidate the interplay between BSi contents and nutrient stoichiometry, lignin and C concentrations of *Phragmites australis* in a broad range of wetlands. Our central hypothesis is that the uptake and assimilation of Si by *Phragmites australis* will regulate nutrient stoichiometry and the synthesis of degradable compounds, with BSi accumulation potentially substituting structural C compounds, especially lignin. This will in turn control the efficacy of blue C storage in wetland ecosystems.

2 Materials and methods

2.1 Study site and plant samples

The study site was situated in the Baiyangdian wetland (N38°–39°, E115°–116°), with an area of 366 km^2. It is an alluvial lowland of the Yongding River and the Hutuo River located in the central region of the North China Plain, within the municipality of Baoding, Hebei Province, China (Figure 1). River sedimentation and human activities have created 143 shallow lakes and

more than 3700 ditches within the Baiyangdian wetland. The average annual precipitation is 563.7 mm with a temperature between 7.3–12.7˚C. The wetlands are 5–10 m above sea level.

In September 2017, aboveground biomass (150–200 g) of five separate *Phragmites australis* plants were sampled using secateurs from each of the 68 sites. The plant samples were placed in plastic bags and stored at 4˚C and returned to the laboratory. Plant samples were manually separated into stems, leaf blades and sheaths, and then washed with ultra-pure water and then dried at 75˚C for 48 h. The dried samples were ground to below 100 mesh size using a micro plant grinding machine.

2.2 Elemental analysis

The total plant C, N and S contents were measured by combustion using an Elementar Vario EL III (Elementar Analysensysteme, GmnH, Germany). For the determination of Si and phosphorus (P), 50 mg plant samples were placed in a porcelain crucible with lithium metaborate and fused at 950˚C for 15 min in a muffle furnace. After cooling to room temperature, fused samples were dissolved with 20 mL of 4% nitric acid (v/v), and then reached a constant volume to 50 mL. The Si content was determined using molybdenum blue colorimetry method (Ru et al., 2018) while P content was determined using ammonium molybdate spectrophotometric method on a UV spectrophotometer (UV-1800, Shimadzu Corporation, Japan) (Lu, 2002).

2.3 Lignin analysis

129 For lignin phenol analysis, plant samples (50 mg) were mixed with 1 g CuO, 100 mg
130 ammonium iron (II) sulfate [$Fe(NH_4)_2(SO_4)_2 \cdot 6H_2O$] and 15 mL of N_2-purged NaOH solution (2
131 mM) in Teflon-lined high pressure vessels. The headspace of the vessels was flushed with N_2 for
132 10 min before being sealed, and heated at 150˚C for 2.5 h in an oven. After these treatments, the
133 lignin macromolecules in samples were broken down into small monomeric phenolic fragments.
134 The lignin oxidation products (LOPs) were spiked in vessels with a surrogate standard (i.e., ethyl
135 vanillin) to calculate sample recovery rate (Otto et al., 2005; Ma et al., 2018).
136 After transfer, vortex, ultrasound and centrifugation, the clarified supernatant was acidified
137 to pH < 2 with 6 mmol L^{-1} HCl, and kept in the dark for 1 h. After centrifugation (4000 r.p.m., 25
138 min), the LOPs were extracted from the clear supernatant with ethyl acetate. The LOPs dissolved
139 in ethyl acetate were then concentrated to dryness under a gentle stream of N_2, and derivatized
140 with N, O-bis-(trimethylsilyl) trifluoroacetamide (BSTFA) and pyridine (70˚C, 3 h) to yield
141 trimethylsilyl (TMS) derivatives for quantification (Zhu et al., 2019).
142 Trimethylsilyl (TMS) derivatives of LOPs were quantified using internal standards on an
143 Agilent 7890B gas chromatograph coupled to an 7010B TQ mass spectrometer (Agilent, USA)
144 using a DB-5MS column (30 m × 0.25 mm × 0.25 μm). A constant current mode was used, with a
145 controlled flow rate of carrier gas (high-purity He; 1.0 mL min^{-1}). Inlet temperature was 300˚C,
146 injection volume was 0.2 μL with split (5: 1) injection and the detector temperature was 280˚C.
147 Oven temperature increased from 65˚C to 300˚C at a rate of 6˚C min^{-1}, and finally held at 300˚C
148 for 5 min. The mass spectrometer was operated in the electron impact mode (EI) at 70 eV and
149 scanned with MRM.

Quantification of the trimethylsilyl (TMS) derivatives of LOPs was accounted for compound loss during the extraction procedures by dividing the recovery of the surrogate standards. Vanillyl (vanillin, acetovanillone, vanillic acid), syringyl (syringaldehyde, acetosyringone, syringic acid), and cinnamyl (*p*-coumaric acid, ferulic acid), and these three types of vanillyl, syringyl, cinnamyl (VSC) phenols were summed to represent lignin in plants. Lignin content was normalized to C content to reflect its relative abundance in plant biomass C.

2.4 Statistical analysis

Linear and logarithmic regression analyses were performed to reveal the relationships between the concentrations or storages of BSi and those of C, N, P, S or VSC. Significant differences in means were analyzed using one-way analysis of variance (ANOVA) followed by Duncan's multiple-range test using SPSS ver. 21.0 software.

Total aboveground biomass and C content were calculated as follows:

$$B_{ab} = B_{st} + B_{le} + B_{sh} \quad (1)$$

$$C_{ab} = \frac{C_{st} \times M_{st} + C_{le} \times M_{le} + C_{sh} \times M_{sh}}{M_{total}} \quad (2)$$

$$S = B \times C \quad (3)$$

Where B_{ab}, B_{st}, B_{le}, and B_{sh} represent total aboveground biomass, stem biomass, leaf biomass, and sheath biomass of *Phragmites australis*, respectively. C_{ab}, C_{st}, C_{le}, and C_{sh} represent the contents of elements in the total aboveground, stem, leaf, and sheath of *Phragmites australis*, respectively. *S*, *B* and *C* represent the storage of different elements, biomass of different tissues, and contents of different elements.

3 Results

3.1 Variations in nutritional parameters of samplings sites

The concentrations of dissolved Si in surface water (0–40 cm) was in the range of 0.49–11.73 mg L^{-1}, with the mean value of 4.78 ± 2.71 mg L^{-1} (Figure 2A). Correspondingly, the concentrations of dissolved Si in topsoil (0–20 cm) ranged from 0.10 to 0.80 mg g^{-1}, with the mean value of 0.35 ± 0.13 mg g^{-1} (Figure 2B). TN ranged from 0.40 to 6.17 mg L^{-1}, with mean of 1.25 ± 0.80 mg L^{-1}, and inorganic N of NH_4^+ and NO_3^- was 0.23 ± 0.06 mg L^{-1} and 0.19 ± 0.09 mg L^{-1}, respectively (Figure 2C). TP and PO_4^{3-} varied in ranges of 0.00–0.44 mg L^{-1} (0.07 ± 0.07 mg L^{-1}) and 0.01–0.43 mg L^{-1} (0.02 ± 0.05 mg L^{-1}) in all sampling sites (Figure 2D). Computationally, differences in N: P ratios were widely distributed.

3.2 Elemental composition in different tissues of Phragmites australis

BSi concentrations differed between different tissues of *Phragmites australis*, increasing from the stem (0.214 ± 0.096 mmol g^{-1}) to leaf (0.867 ± 0.309 mmol g^{-1}) and sheath (0.903 ± 0.427 mmol g^{-1}). C concentrations decreased from stem (38.378 ± 0.378 mmol g^{-1}) to leaf (36.343 ± 0.827 mmol g^{-1}) and sheath (35.883 ± 1.175 mmol g^{-1}). The concentrations of N and P in leaf (N = 1.988 ± 0.228 mmol g^{-1}; P = 0.056 ± 0.010 mmol g^{-1}) were greater than in the stem (N = 0.624 ± 0.171 mmol g^{-1}; P = 0.018 ± 0.009 mmol g^{-1}) and sheath (N = 0.693% ± 0.086 mmol g^{-1}; P = 0.023 ± 0.007 mmol g^{-1}). The S concentrations in leaf and sheath were similar, with

191 a mean value of 0.123 ± 0.031 mmol g^{-1} and 0.074 ± 0.021 mmol g^{-1}, respectively, and the lowest
192 S concentration was measured in stem (0.024 ± 0.009 mmol g^{-1}).

193 The average molar ratios of BSi/C, BSi/N and BSi/P and BSi/S in the tissues of *Phragmites*
194 *australis* were stem < leaf < sheath, and followed the order of BSi/C < BSi/N < BSi/S < BSi/P in
195 three different tissues. In addition, the BSi/C, BSi/N, BSi/P, BSi/S ratios have the same variation
196 tendency in the tissues of *Phragmites australis*, followed the order of stem < leaf < sheath (Table
197 1).

198

199 *3.3 Relationships between BSi and C, N, P and S*

200 There is a significant negative correlation between BSi and C concentration in the leaf (R^2 =
201 0.60, $p < 0.001$) and sheath ($R^2 = 0.44$, $p < 0.001$) of *Phragmites australis.* Similarly, N and P
202 contents were weakly negatively related to BSi in leaf (N: $R^2 = 0.16$, $p < 0.01$; P: $R^2 = 0.09$, $p <$
203 0.05) and sheath (N: $R^2 = 0.06$, $p < 0.05$; P: $R^2 = 0.07$, $p < 0.05$) (Figure 3A). In contrast to these
204 negative correlations, the BSi and S are weakly positively correlated in leaf ($R^2 = 0.10$, $p = 0.01$)
205 and stem ($R^2 = 0.05$, $p = 0.071$) (Figure S3 & S4). For the stem, there were no significant
206 relationships between BSi and C, N, P, or S (Figure S2). Only C concentration was negatively
207 correlated with BSi concentration ($R^2 = 0.27$, $p < 0.001$) in aboveground biomass of *Phragmites*
208 *australis*, with no significant relationships with N, P and S concentrations (Figure S1). BSi
209 accumulation was positively logarithmically correlated with the total biomass of C, N, P and S in
210 the stem (Figure S2E-H), leaf (Figure S3E-H), sheath (Figure S4E-H) and aboveground biomass
211 (Figure S1E-H) of *Phragmites australis* at the level of the individual plant (Figure 3B).

212

213 *3.4 Relationships between BSi and lignin-derived phenols*

214 The BSi concentrations were in the range of 0.072–0.816 mmol g^{-1} (stem), 0.313–2.052

215 mmol g^{-1} (leaf), and 0.264–2.362 mmol g^{-1} (sheath), respectively (Table 1). The concentrations of

216 the C-normalized sum of VSC phenols were 66.763–120.670 mg g^{-1} C in stem, 36.439–55.905

217 mg g^{-1} C in leaf, and 65.400–114.118 mg g^{-1} C in sheath, respectively. The average content of

218 C-normalized VSC phenols decreased in the order of stem (97.613 mg g^{-1} C) > sheath (83.332

219 mg g^{-1} C) > leaf (47.552 mg g^{-1} C). BSi concentrations were significantly negatively correlated to

220 those of C-normalized VSC phenols in stems (R^2 = 0.47, p < 0.001) and sheaths (R^2 = 0.46, p <

221 0.001), but the relationship was not significant in leaves (p > 0.05) (Figure 4).

222

223 **4 Discussion**

224 *4.1 Si biogeochemistry and its effect on nutrient accumulation and cycles*

225 BSi contents of *P. australis* ranged from 0.068 to 0.901 mmol g^{-1}DW (Table 1), and are

226 comparable with concentrations ranging from 0.071–1.000 mmol g^{-1}DW reported previously for

227 13 wetland species (Schoelynck et al., 2010). The variation in BSi contents may reflect the

228 difference in mechanical and photosynthetic function of Si (Sivanesan and Park, 2014). The

229 content of BSi increased in the order of stem < leaf ⩽ sheath, suggesting that *P. australis* cannot

230 avoid Si uptake and transpiration-driven transport to aboveground parts (Cooke and Leishman,

231 2011). The high Si contents in the aboveground parts of *P. australis* sampled from the studied

232 wetland further confirm that *this* species has a high capacity to accumulate BSi (Struyf et al.,

2007). Since *P. australis* covers large areas meadow grassland, freshwater marshes, estuaries, and coastlines (e.g., salt marshes), and has a high net primary production (up to 6000 g m^{-2} yr^{-1}) (Rejmankova, 2011), the large storage of BSi in *P. australis* represents a major component in the Si cycle in wetland ecosystems.

Wetlands are characterized by active biogeochemical cycling of Si, exhibiting strong control on catchment scale Si fluxes (Struyf and Conley, 2009; 2012; Borrelli et al., 2012), and a strong impact on source and sink for Si from plants has been highlighted (e.g., Struyf et al., 2005, 2007, 2010; Opdekamp et al., 2012). Owing to the annual defoliation and decomposition of *P. australis* in autumn and winter, the stored BSi can also be released through biomass decomposition, while uptake occurs during net primary productivity. It has been demonstrated that 50% of BSi in *P. australis* can be dissolved within 14 days in tidal marshes (Struyf et al., 2007). Similarly, diatoms absorb Si in spring and summer, forming a seasonal cycle of BSi in wetlands (Conley and Carey, 2015; Zang et al., 2016). Thus, the subsequent transport (in the form of dissolved Si) downstream will depend on the dissolution rate of macrophyte BSi.

For different tissues, BSi was significantly negatively correlated with N and P in both the leaf and sheath, but not in the stem. This may be because leaf and sheath have a photosynthetic function, resulting in higher N and P demands by the leaf and sheath. The accumulation of BSi promotes biomass storage of N and P storage in all three tissues, likely through enhancing N and P uptake efficiency and thus improving plant biomass (Figure 5B & S6). Neu et al. (2017) showed that nutrient use efficiency was improved at a whole-plant level by Si through enhanced biomass production. The negative correlation between N and Si was also shown for terrestrial

254 grasses (Song et al., 2014) and wheat (Murozuka et al., 2014). This may be explained by a
255 decrease in Si accumulation under higher N availability (Wallace et al., 1976). Based on
256 phylogenetics for both the terrestrial (Wallace et al., 1976) and emergent plants (Schaller et al.,
257 2016), grasses would accumulate less Si under high N demand. This is in line with our findings
258 for *P. australis* that leaf and sheath accumulated less Si as N content increased (Figure S3 & S4).
259 Contrary to our results, BSi concentrations have been shown to be positively correlated with P in
260 grass (Eneji et al., 2008), reeds (Schaller et al., 2012a) and wheat (Kostic et al., 2017; Neu et al.,
261 2017). These experiment findings were to increase Si availability from Si fertilizer application,
262 which need further investigations in field scale. In soils, Si availabilities were significantly
263 positive correlated to P mobilization in arctic soils, and laboratory experiments further confirmed
264 this effect (Schaller et al., 2019). Si, albeit not an essential element for plant growth, interferes
265 with P metabolism and plant nutrient status (Eneji et al., 2008), and it perhaps exerts either a
266 positive or negative effect depending on the levels of Si and other nutrients supply for plants in
267 different soil conditions.
268
269 *4.2 A trade-off between structural components*
270 The antagonistic relationship between BSi and C in aboveground compartments of *P.*
271 *australis* are shown in Figure 3 and Table 2. Similar relationships were also found in other
272 wetland species (Schaller et al., 2016), Si-fertilized winter wheat (Neu et al., 2017) and reeds
273 (Schaller et al., 2012a; 2012b), plant communities grown on different soil types (Cooke and
274 Leishman, 2012) and field-grown rice straw (Klotzbücher et al., 2018). Two hypotheses are

proposed to explain this relationship: (i) BSi might dilute the C concentration, i.e., all elements necessarily decrease accompanied with increase in BSi concentrations; (ii) BSi incorporated in plants could substitute C and play similar physiological and ecological function.

The weak negative correlations between BSi and N or P in leaf and sheath tissue supports the 'dilution effect' (Figure S3 & S4). However, BSi was not correlated to total N and P content of the aboveground biomass of *P. australis* ($p < 0.001$) (Figure S1). Furthermore, BSi had a significant positive relationship with S in both leaf and sheath, but not in stem or the whole aboveground biomass of *P. australis* (Figure S1, S2, S3 & S4). These features may contradict the 'dilution effect' of Si incorporation, which would decrease the abundance of C and other elements with a similar magnitude.

The negative linear relationships between the concentrations of BSi and VSC phenols in stem and sheath imply that Si availability could influence the composition of organic matter produced by *P. australis* in the sampled wetlands, with reduced lignin when Si content increases. The substitution of structural C by Si as suggested by Raven (1983) was first proposed for *P. australis* in a single species experiment. When bioavailable Si is transported to aboveground compartments that are involved in transpiration, it irreversibly polymerizes as amorphous silica gel ($SiO_2 \cdot nH_2O$) in cell walls and phytoliths. Importantly, synthesizing structural C compounds (e.g., lignin) requires 10–20 times more energy than incorporating structural SiO_2 (calculated on basis of material weight) (Raven, 1983). It has been shown that an increase in plant Si content by 1%, on average, causes a C biomass reduction of between 1.26% to 5.87% (Neu et al., 2017; Klotzbücher et al., 2018). Studies on the trade-off between reduced biomass C and increased Si

296 level indicate that Si fertilizer application enhances C accumulation in plant biomass (Li et al.,
297 2018). These processes are further supported by our data on biomass C concentration and VSC
298 phenols, which showed that *P. australis* grown in wetlands with the lowest Si concentration
299 produced about 10%–30% more C and lignin per mass than the plants with the highest Si
300 concentration.

301 Lignin is one of the most important structural C compounds, Si-mediated reductions in
302 lignin biosynthesis has been highlighted not only on food crops such as rice (*Oryza sativa*)
303 (Suzuki et al., 2012; Klotzbücher et al., 2018), wheat (*Triticum aestivum*) (Murozuka et al., 2014),
304 but also on cash crops such as canola (*Brassica napus*) (Hashemi et al., 2010) and tobacco
305 (*Nicotiana rustica*) (Hajiboland et al., 2017); Further, a negative relationship between Si and
306 lignin concentration for different wetland species has been shown (Schoelynck et al., 2010).
307 These studies demonstrated that both monocots and dicots have significant negative correlations
308 between the concentrations of Si and those of lignin in leaves and straw, especially under stress
309 conditions. These observations suggest that the incorporation of structural Si represents an
310 economic strategy of plants to confront a range of environmental stresses. If Si accumulation is
311 linearly related to biomass C storage, it caused by large differences in individual biomass, this is
312 because the magnitude of biomass is much larger than BSi and C concentrations. In our results,
313 BSi accumulation is logarithmically related to biomass C storage with a threshold (Figure S1).
314 The non-linear nature of this relationship suggests that BSi incorporated into the plants does start
315 to substitute C, especially at higher BSi concentrations.

316 Si is accumulated where has the highest stomata density, because Si is transported with the
317 water and if the water is lost by transpiration, thus the Si will participate (Katz, 2019; Coskun et
318 al., 2019). For three different tissues, we found BSi was significantly negatively related to C in
319 both leaf and sheath, and to VSC phenols in stem and sheath. This may be related to the different
320 morphological and physiological functions (e.g., stomatal conductance) of these plant tissues.
321 Leaf is the photosynthetic tissue with highest stomata density, while stem exerts the mechanical
322 support with lowest stomata density, and sheath has both a stabilization function and is
323 photosynthetically active (Feng et al., 2008). The concentration of VSC phenols were the lowest
324 in leaves and are weakly negatively related to BSi, suggesting excessive silicification and
325 lignification might affect the efficiency of plant photosynthesis (Coskun et al., 2016). The
326 significant negative relationships between BSi and VSC phenols in the stem and sheath might
327 reflect that Si (a) has a similar function to lignin, promoting upright stature and resistance to
328 lodging (flattening by wind or rain), especially for wetland plants (Schoelynck and Struyf, 2016);
329 and (b) can act as a metabolically 'cheaper' structural substitute for C. It has been suggested that
330 such a substitution could have evolved particularly at times when CO_2 concentrations were low,
331 such as during the Miocene (Cooke and Leishman, 2011). The latter processes are further
332 supported by our results that no correlations between BSi and VSC phenols were observed for the
333 leaf of *P. australis* receiving more CO_2 and light energy than stem and sheath during
334 photosynthesis. Hence, C compounds (a high energy demand during formation) substituted by Si
335 (a low energy requirement for uptake and storage) under low CO_2 availability and high Si
336 availability may be beneficial for the growth of macrophytes (Raven et al., 1983). Overall, Si

337 seems to affect the C concentration and lignin metabolism depending on the function of the
338 tissues, and the trade-off between productivity and stabilization/defense.

339 The energy 'surplus' available at high-Si supply can be used by plants to synthesize non- or
340 less- C-containing structural compounds, which usually have lower 'production costs' than lignin
341 (De Vries et al., 1974). This could be one reason for the positive effects of Si fertilizer application
342 on biomass production and grain yields reported in many previous studies (e.g., Yamamoto et al.,
343 2012; Zhang et al., 2015; Li et al., 2018). In our results, Si concentrations in *Phragmites*
344 *australis* were not significantly related to biomass production (Figure 5A & S5), given that a
345 multitude of potential drivers for biomass production may have differed across the study sites;
346 including soil, water table, contaminant stress, other nutrient elements, etc (Figure 2). However,
347 Si accumulation was positively logarithmical related to biomass production (Figure 5B & S6).
348 Thus, BSi improved overall nutrient use efficiency and lowered the synthesis of lignin, leading to
349 the increased primary productivity of *Phragmites australis*. Trade-off analyses for decreases in C
350 and lignin concentration versus increase in BSi concentration and biomass production in response
351 to BSi availability at the individual level or even ecosystem level needs to be further evaluated.
352
353 *4.3 Implications of litter composition and quality to silicon-carbon coupled cycles along the*
354 *land-ocean continuum*

355 Wetlands have a great potential for C sequestration and storage under hydric conditions
356 (Abril et al., 2014). The rate of mineralization of biomass to CO_2 and/or CH_4 controls the C
357 sequestration in these systems (Gessner et al., 2010; Cotrufo et al., 2015; Zukswert and Prescott,

358 2017). Lignin is one of the most resistant C components and is thought to form a 'protective
359 shield' around more labile cell wall compounds, such as cellulose, hemicellulose, and protein
360 (Talbot and Treseder, 2012), thus contributing to the preservation of these compounds (Berg and
361 McClaugherty, 2003; Vänskä et al., 2016). Hence, lignin often retards litter decay (Talbot and
362 Treseder, 2012; Zhang et al., 2008), especially under anoxic conditions, e.g., wetlands or paddy
363 soils (Bierke et al., 2008).

364 One of the most well-established patterns in ecosystem ecology is that litter decomposition
365 rates are correlated with the initial ratios of C: N, lignin: N, and lignin: cellulose in litters
366 (Bradford et al., 2016; Chomel et al., 2016; García-Palacios et al., 2016). In our study, BSi altered
367 nutrient stoichiometry (C: N: P: S) and reduced lignin synthesis. Based on a meta-analysis, the
368 lignin content and litter decomposition rate have a significantly negative relationship ($p < 0.001$)
369 from different plant species (Zhang et al., 2008; Sun et al., 2018; Figure 6). Zhang et al. (2008)
370 reported that the chemical traits of litter account for over 73% of the variation in litter
371 decomposition rates. Therefore, BSi may provide a direct or indirect effect regulating litter
372 chemistry traits and quality, which play an important role in influencing the decomposition
373 kinetics and the flow of organic matter between C pools.

374 Given that BSi was negatively correlated with lignin and macrophytes have an overlooked
375 but potentially vast storage capacity for Si, it is important to understand their role as silica sinks
376 along the land-ocean continuum (Figure 7). It has been reported that Si concentrations are
377 positively correlated with rates of C loss during plant litter decomposition for *Phragmites*
378 *australis* (Schaller and Struyf, 2013; Schaller et al., 2014). Marxen et al. (2016) also reported that

379 the C loss from high-Si rice straw (~12% of the dry weight) was about 10%–15% higher than the
380 C loss from low-Si rice straw (~5%) after 33 days of decomposition in a waterlogged soil,
381 implying that C turnover might directly related to differences in lignin synthesis regulated by BSi
382 concentration in rice straw. Therefore, the reason for the altered decomposition rate are linked to
383 changes in the quality of the organic matter, specifically the structural C compounds of plants,
384 which in turn is influenced by Si. Therefore, the role of Si availability in controlling composition
385 and quality of macrophyte litter may have an important impact on C cycling in wetlands (Conley,
386 2002; Street-Perrott and Barker, 2008; Figure 2 and Figure 7).
387
388 *4.4 Sustainable wetland management to increase biogeochemical C sequestration*
389 Silicon is one of the major nutrient elements for wetlands, estuarine and coastal ecosystems,
390 which often plays important roles in macrophyte growth and community structure (Schoelynck
391 and Struyf, 2016). Influence in plant Si uptake, release, and recycling can be affected by nutrient
392 availability (eutrophication and/or fertilizer), human management (e.g. grazing, harvesting) and
393 vegetation composition (Engloner, 2009). Emsens et al. (2016) reported that eutrophication had
394 stimulatory effects on total Si storage in wetland vegetation (following an increase in biomass
395 production), and eutrophication-induced shifts in feedbacks on litter decomposition rate are likely
396 to increase rates of Si cycling. The authors further deduced that eutrophication may thus facilitate
397 high rates of net Si export from coastal wetlands to the oceans. However, this hypothesis needs to
398 be testified in natural ecosystems. In addition, the application of Si fertilizer is becoming more
399 common (Bocharnikova et al., 2010; Haynes, 2014; Tubana et al., 2016). Based on a

meta-analysis of the control and the treatment of Si application, Li et al. (2018) reported that Si-mediated recovery generally increases plant biomass C by 35% and crop yield by 24% under abiotic and biotic stresses. Some adverse conditions, including salt stress, nutritional imbalance, waterlogged, bacterial blight, brown spot, stalk borer, are common phenomenon in wetlands (Otte, 2001; Engloner, 2009). Thus, additional Si supply and the subsequent increase in biogeochemical Si cycle could alleviate the adverse effects of abiotic and biotic stresses and thus accelerate biomass C accumulation in wetlands. Concurrently, macrophytes were used in the application of agricultural and industrial production and the prevention of fire, people usually harvest macrophytes because of its economic value and the implementation of wetland management policies (Valkama et al., 2008). It cannot be ignored that human intensification caused a reduction of Si availabilities in soils due to large exports of straw residuals over the last decades (Meharg and Meharg, 2015; Tubana et al., 2016), and little attention has been given to the Si pool and its effect on ANPP and ecosystem resilience. Different vegetation composition largely varies in Si content in wetlands (Li et al., 2013b), and ANPP is also largely different for various types of macrophytes (Rejmankova, 2011). There is an increasing topic that *Spartina alterniflora* invasion can strongly influence Si distribution (Zhai and Xue, 2016) and C cycling processes (Yuan et al., 2019), thus it may affect climate change by changing C sequestration and greenhouse gas emissions in the invaded wetlands.

Si cycling in plant-soil systems both promotes C accumulation in plant biomass (Detmann et al., 2012; Kang et al., 2016; Marxen et al., 2016; Song et al., 2016), and mediates the plant quality for litter decomposition after shoot senescence and death (Rejmankova and Houdkova,

421 2006). Therefore, Si availability might not only affect the Si cycle and recycle, but also affect C
422 cycling over large spatial scales (Derry et al., 2005; Struyf et al., 2005). Given that external
423 changes (climate, vegetation community, harvest practices, fertilizer, etc.) are likely to alter Si
424 availabilities in many regions of the world, and this may have profound consequences for C
425 cycling in ecosystems dominated by Si-accumulating plants that are primarily the members of the
426 *Poaceae* family, including rice, wheat, sugarcane, and barley (Ma et al., 2001). Si nutrition might
427 thus exert crucial but hardly evaluated functions in a wide range of ecosystems, including
428 wetlands, bamboo forests, grasslands, and most agricultural systems. However, Si is not yet
429 considered a factor in conceptual models on terrestrial C cycling (Schmidt et al., 2011; Lehmann
430 and Kleber, 2015). This might be a major shortcoming, especially with respect to C cycling in
431 ecosystems dominated by Si-accumulating plants. Therefore, Si management is essential in
432 simultaneously regulating biogeochemical cycles of carbon and nutrients in natural ecosystems.
433
434 **5 Conclusions**

435 We have shown that *Phragmites australis* contains significant amounts of BSi with its
436 concentration differing between plant compartments. BSi concentration had a negative
437 relationship with lignin in the stem and sheath tissues supporting the notion that Si substitutes
438 structural C components in *Phragmites australis*. Furthermore, we showed that the BSi
439 concentration was negatively correlated with the C concentration in aboveground biomass of
440 *Phragmites australis*, but that high BSi accumulation indeed resulted in greater net primary
441 productivity, thus resulting in greater plant C storage in the wetland system. On the other hand,

the changes of litter composition in nutrient stoichiometry and reductions in lignin concentrations may provide a possibility for the factors affecting litter decomposition and therefore affects overall C fixation in these systems. Hence, Si-mediated processes which increase biomass production and litter quality, may play an important role in the biogeochemical C cycle, especially in wetlands dominated by Si-accumulating plants.

Acknowledgements

This study was financially supported by the National Natural Science Foundation of China (Grant Nos. 41930862, 41571130042, and 41522207) and the State's Key Project of Research and Development Plan of China (Grant Nos. 2016YFA0601002 and 2017YFC0212700). We thank technical staff Xiaoli Fu for assistance with the establishment of lignin measurement method, and thank Ms. Weihua Yang and Dr. Xiaodong Zhang for assistance with field sampling.

Conflict of interest

All authors declare no conflict of interests.

References

Abril, G., Martinez, J. M., Artigas, L. F., Moreira-Turcq, P., Benedetti, M. F., Vidal, L., Meziaane, T., Kim, J.H., Bernardes, M. C., Savoye, N., Deborde, J., Souza, E. L., Albéric, P., de Souze, M. F. L., Roland, F., 2014. Amazon River carbon dioxide outgassing fuelled by wetlands. Nature, 505(7483), 395.

Ahmed, M., Qadeer, U., Ahmed, Z. I., Hassan, F. U. 2016. Improvement of wheat (*Triticum aestivum*) drought tolerance by seed priming with silicon. Arch. Agron. Soil. Sci., 62(3), 299-315.

Atwood, T. B., Connolly, R. M., Ritchie, E. G., Lovelock, C. E., Heithaus, M. R., Hays, G. C., ... & Macreadie, P. I., 2015. Predators help protect carbon stocks in blue carbon ecosystems. Nat. Clim. Change, 5(12), 1038-1045.

Berg, B., McClaugherty, C., 2003. Plant litter: decomposition, humus formation, carbon sequestration. Springer-Verlag, Berlin, Germany.

Bierke, A., Kaiser, K., Guggenberger, G., 2008. Crop residue management effects on organic matter in paddy soils—the lignin component. Geoderma, 146(1-2), 48-57.

Bocharnikova, E. A., Loginov, S. V., Matychenkov, V. V., Storozhenko, P. A., 2010. Silicon fertilizer efficiency. Rus. Agri. Sci., 36(6), 446-448.

Borrelli, N., Osterrieth, M., Romanelli, A., Alvarez, M. F., Cionchi, J. L., Massone, H., 2012. Biogenic silica in wetlands and their relationship with soil and groundwater biogeochemistry in the Southeastern of Buenos Aires Province, Argentina. Environ. Earth. Sci., 65(2), 469-480.

Bosnic, P., Bosnic, D., Jasnic, J., Nikolic, M., 2018. Silicon mediates sodium transport and partitioning in maize under moderate salt stress. Environ. Exp. Bot., 155, 681-687.

Bradford, M. A., Berg, B., Maynard, D. S., Wieder, W. R., Wood, S. A., 2016. Understanding the dominant controls on litter decomposition. J. Ecol., 104(1), 229-238.

Castellano, M. J., Mueller, K. E., Olk, D. C., Sawyer, J. E., Six, J., 2015. Integrating plant litter quality, soil organic matter stabilization, and the carbon saturation concept. Global Change Biol., 21(9), 3200-3209.

Chomel, M., Guittonny-Larchevêque, M., Fernandez, C., Gallet, C., DesRochers, A., Paré, D., Jackson, B. G., Baldy, V., 2016. Plant secondary metabolites: a key driver of litter decomposition and soil nutrient cycling. J. Ecol., 104(6), 1527-1541.

Conley, D. J., 2002. Terrestrial ecosystems and the global biogeochemical silica cycle. Global Biogeochem. Cy., *16*(4), 68-1.

Conley, D. J., Carey, J. C., 2015. Biogeochemistry: Silica cycling over geologic time. Nat. Geosci., 8(6), 431.

Cooke, J., & Leishman, M. R., 2011. Is plant ecology more siliceous than we realise?. Trends Plant Sci., 16(2), 61-68.

Cooke, J., Leishman, M. R., 2011. Silicon concentration and leaf longevity: is silicon a player in the leaf dry mass spectrum? Funct. Ecol., 25(6), 1181-1188.

Cooke, J., Leishman, M. R., 2012. Tradeoffs between foliar silicon and carbon-based defences: evidence from vegetation communities of contrasting soil types. Oikos, 121(12), 2052-2060.

Coskun, D., Britto, D. T., Huynh, W. Q., Kronzucker, H. J., 2016. The role of silicon in higher plants under salinity and drought stress. Front Plant Sci., 7, 1072.

Coskun, D., Deshmukh, R., Sonah, H., Menzies, J. G., Reynolds, O., Ma, J. F., ... & Bélanger, R. R., 2019. The controversies of silicon's role in plant biology. New Phytol., 221(1), 67-85.

503 Cotrufo, M. F., Soong, J. L., Horton, A. J., Campbell, E. E., Haddix, M. L., Wall, D. H., Parton, W. J., 2015.
504 Formation of soil organic matter via biochemical and physical pathways of litter mass loss. Nat.
505 Geosci., 8(10), 776.
506 De Vries, F. P., Brunsting, A. H. M., Van Laar, H. H., 1974. Products, requirements and efficiency of
507 biosynthesis a quantitative approach. J. Theor. Biol., 45(2), 339-377.
508 Derry, L. A., Kurtz, A. C., Ziegler, K., Chadwick, O. A., 2005. Biological control of terrestrial silica cycling
509 and export fluxes to watersheds. Nature, 433(7027), 728-731.
510 Detmann, K. C., Araújo, W. L., Martins, S. C., Sanglard, L. M., Reis, J. V., Detmann, E., Rodrigues, F. Á.,
511 Nunes-Nesi, A., Fernie, A. R., DaMatta, F. M., 2012. Silicon nutrition increases grain yield, which, in turn,
512 exerts a feed-forward stimulation of photosynthetic rates via enhanced mesophyll conductance and alters
513 primary metabolism in rice. New Phytol., 196(3), 752-762.
514 Emsens, W. J., Schoelynck, J., Grootjans, A. P., Struyf, E., van Diggelen, R., 2016. Eutrophication alters Si
515 cycling and litter decomposition in wetlands. Biogeochemistry, 130(3), 289-299.
516 Eneji, A. E., Inanaga, S., Muranaka, S., Li, J., Hattori, T., An, P., Tsuji, W., 2008. Growth and nutrient use in
517 four grasses under drought stress as mediated by silicon fertilizers. J. Plant Nutr., 31(2), 355-365.
518 Engloner, A. I., 2009. Structure, growth dynamics and biomass of reed (*Phragmites australis*)–A
519 review. Flora-Morphology, Distribution, Functional Ecology of Plants, 204(5), 331-346.
520 Feng, D. L., Yang, J., Liu, Y., Xie, J., & Zhong, Z. C., 2008. Photosynthesis and chlorophy II fluorescence
521 parameters of the reed (*Phragmites communis*) grown in the hydro-fluctuation belt of Three Gorges
522 Reservoir Area. Acta Ecologica Sinica, 28(5), 2013-2021.
523 Fioretto, A., Di Nardo, C., Papa, S., Fuggi, A., 2005. Lignin and cellulose degradation and nitrogen dynamics
524 during decomposition of three leaf litter species in a Mediterranean ecosystem. Soil Biol. Biochem., 37(6),
525 1083-1091.
526 García-Palacios, P., McKie, B. G., Handa, I. T., Frainer, A., Hättenschwiler, S., 2016. The importance of litter
527 traits and decomposers for litter decomposition: a comparison of aquatic and terrestrial ecosystems within
528 and across biomes. Funct. Ecol., 30(5), 819-829.
529 Gessner, M. O., Swan, C. M., Dang, C. K., McKie, B. G., Bardgett, R. D., Wall, D. H., Hättenschwiler, S., 2010.
530 Diversity meets decomposition. Trends Ecol. Evol., 25(6), 372-380.
531 González-Alcaraz, M. N., Egea, C., Jiménez-Cárceles, F. J., Párraga, I., Maria-Cervantes, A., Delgado, M. J.,
532 Álvarez-Rogel, J., 2012. Storage of organic carbon, nitrogen and phosphorus in the soil–plant system of
533 Phragmites australis stands from a eutrophicated Mediterranean salt marsh. Geoderma, 185, 61-72.
534 Hajiboland, R., Bahrami-Rad, S., Poschenrieder, C., 2017. Silicon modifies both a local response and a
535 systemic response to mechanical stress in tobacco leaves. Biol. Plantarum., 61(1), 187-191.
536 Hashemi, A., Abdolzadeh, A., Sadeghipour, H. R., 2010. Beneficial effects of silicon nutrition in alleviating
537 salinity stress in hydroponically grown canola, *Brassica napus* L., plants. Soil. Sci. Plant Nutr., 56(2),
538 244-253.
539 Hättenschwiler, S., Jørgensen, H. B., 2010. Carbon quality rather than stoichiometry controls litter
540 decomposition in a tropical rain forest. J. Ecol., 98(4), 754-763.
541 Haynes, R. J., 2014. A contemporary overview of silicon availability in agricultural soils. J. Plant Nutr. Soil Sci.,
542 177(6), 831-844.

He, M., Zhao, R., Tian, Q., Huang, L., Wang, X., Liu, F., 2019. Predominant effects of litter chemistry on lignin degradation in the early stage of leaf litter decomposition. Plant Soil, 1-17.

Hou, L., Liu, M., Yang, Y., Ou, D., Lin, X., Chen, H., 2010. Biogenic silica in intertidal marsh plants and associated sediments of the Yangtze Estuary. J. Environ. Sci., 22(3), 374-380.

Imtiaz, M., Rizwan, M. S., Mushtaq, M. A., Ashraf, M., Shahzad, S. M., Yousaf, B., Saeed, D. A., Rizwan, M., Nawaz, M. A., Mehmood, S., Tu, S., 2016. Silicon occurrence, uptake, transport and mechanisms of heavy metals, minerals and salinity enhanced tolerance in plants with future prospects: a review. J. Environ. Manage., 183, 521-529.

Kang, J., Zhao, W., Zhu, X., 2016. Silicon improves photosynthesis and strengthens enzyme activities in the C3 succulent xerophyte *Zygophyllum xanthoxylum* under drought stress. J. Plant Physiol., 199, 76-86.

Katz, O., 2019. Silicon content is a plant functional trait: implications in a changing world. Flora, 254, 88-94.

Klotzbücher, T., Klotzbücher, A., Kaiser, K., Vetterlein, D., Jahn, R., Mikutta, R., 2018. Variable silicon accumulation in plants affects terrestrial carbon cycling by controlling lignin synthesis. Global Change Biol., 24(1), e183-e189.

Kostic, L., Nikolic, N., Bosnic, D., Samardzic, J., Nikolic, M., 2017. Silicon increases phosphorus (P) uptake by wheat under low P acid soil conditions. Plant Soil, 419(1-2), 447-455.

Krauss, K. W., Noe, G. B., Duberstein, J. A., Conner, W. H., Stagg, C. L., Cormier, N., Jones, M. C., Bernhardt, C. E., Lockaby, B. G., From, A. S., Doyle, T. W., Day, R. H., Ensign, S. H., Pierfelice, K. N., Hupp, C. R., Chow, A. T., Whitbeck, J. L., 2018. The role of the upper tidal estuary in wetland blue carbon storage and flux. Global Biogeochem. Cy., 32(5), 817-839.

Laing, M. D., Gatarayiha, M. C., Adandonon, A., 2006. Silicon use for pest control in agriculture: a review. In Proceedings of the South African Sugar Technologists' Association, 80, 278-286.

Lehmann, J., Kleber, M., 2015. The contentious nature of soil organic matter. Nature, 528(7580), 60.

Li, Z., Song, Z., Li, B., 2013a. The production and accumulation of phytolith-occluded carbon in Baiyangdian reed wetland of China. Appl. Geochem., 37, 117-124.

Li, Z., Song, Z., Li, B., Cai, Y., 2013b. Phytolith production in wetland plants of the Hangzhou Xixi Wetlands ecosystem. Journal of Zhejiang A&F University, 30(4), 470-476.

Li, Z., Song, Z., Yan, Z., Hao, Q., Song, A., Liu, L., Yang, X., Xia, S., Liang, Y., 2018. Silicon enhancement of estimated plant biomass carbon accumulation under abiotic and biotic stresses. A meta-analysis. Agron. Sustain. Dev., 38(3), 26.

Liang, Y., Nikolic, M., Bélanger, R., Gong, H., Song, A., 2015. Silicon biogeochemistry and bioavailability in soil. In Silicon in Agriculture (pp. 45-68). Springer, Dordrecht.

Lu, R., 2000. Analytical methods of soil agrochemistry. Beijing, China: China Agricultural Science and Technology Press.

Ma, J. F., Miyake, Y., Takahashi, E., 2001. Silicon as a beneficial element for crop plants. In Studies in Plant Science (Vol. 8, pp. 17-39). Elsevier.

Ma, T., Zhu, S., Wang, Z., Chen, D., Dai, G., Feng, B., Su, X., Hu, H., Li, K., Han, W., Liang, C., Bai, Y., Feng, X., 2018. Divergent accumulation of microbial necromass and plant lignin components in grassland soils. Nat. Commun., 9(1), 3480.

Marxen, A., Klotzbücher, T., Jahn, R., Kaiser, K., Nguyen, V. S., Schmidt, A., Schädler, M., Vetterlein, D., 2016. Interaction between silicon cycling and straw decomposition in a silicon deficient rice production system. Plant Soil, 398(1-2), 153-163.

Meharg, C., Meharg, A. A., 2015. Silicon, the silver bullet for mitigating biotic and abiotic stress, and improving grain quality, in rice? Environ. Exp. Bot., 120, 8-17.

Mitsch, W. J., Bernal, B., Nahlik, A. M., Mander, Ü., Zhang, L., Anderson, C. J., Jørgensen, S. E., Brix, H., 2013. Wetlands, carbon, and climate change. Landscape Ecol., 28(4), 583-597.

Murozuka, E., Laursen, K. H., Lindedam, J., Shield, I. F., Bruun, S., Magid, J., Møller, I. S., Schjoerring, J. K., 2014. Nitrogen fertilization affects silicon concentration, cell wall composition and biofuel potential of wheat straw. Biomass and Bioenergy, 64, 291-298.

Nahlik, A. M., Fennessy, M. S., 2016. Carbon storage in US wetlands. Nat. Commun., 7(1), 1-9.

Neu, S., Schaller, J., Dudel, E. G., 2017. Silicon availability modifies nutrient use efficiency and content, C: N: P stoichiometry, and productivity of winter wheat (*Triticum aestivum* L.). Sci. Rep., 7, 40829.

Opdekamp, W., Teuchies, J., Vrebos, D., Chormański, J., Schoelynck, J., Van Diggelen, R., Meire, P., Struyf, E., 2012. Tussocks: biogenic silica hot-spots in a riparian wetland. Wetlands, 32(6), 1115-1124.

Otte, M. L., 2001. What is stress to a wetland plant?. Environ. Exp. Bot., 46(3), 195-202.

Otto, A., Shunthirasingham, C., Simpson, M. J., 2005. A comparison of plant and microbial biomarkers in grassland soils from the Prairie Ecozone of Canada. Org. Geochem., 36(3), 425-448.

Raven, J. A., 1983. The transport and function of silicon in plants. Biol. Rev., 58(2), 179-207.

Rejmankova, E., 2011. The role of macrophytes in wetland ecosystems. J. Ecol. Environ., 34(4), 333-345.

Rejmánková, E., Houdková, K., 2006. Wetland plant decomposition under different nutrient conditions: what is more important, litter quality or site quality? Biogeochemistry, 80(3), 245-262.

Rogers, K., Kelleway, J. J., Saintilan, N., Megonigal, J. P., Adams, J. B., Holmquist, J. R., Lu, M., Schile-Beers, L., Zawadzki, A., Mazumder, D., Woodroffe, C. D., 2019. Wetland carbon storage controlled by millennial-scale variation in relative sea-level rise. Nature, 567(7746), 91.

Ru, N., Yang, X., Song, Z., Liu, H., Hao, Q., Liu, X., Wu, X., 2018. Phytoliths and phytolith carbon occlusion in aboveground vegetation of sandy grasslands in eastern Inner Mongolia, China. Sci. Total Environ., 625, 1283-1289.

Ruhland, C. T., Remund, A. J., Tiry, C. M., Secott, T. E., 2018. Litter decomposition of three lignin-deficient mutants of Sorghum bicolor during spring thaw. Acta Oecol., 91, 16-21.

Saltonstall, K., 2002. Cryptic invasion by a non-native genotype of the common reed, *Phragmites australis*, into North America. P. Natl. Acad. Sci., 99(4), 2445-2449.

Schaller, J., Brackhage, C., Dudel, E. G., 2012b. Silicon availability changes structural carbon ratio and phenol content of grasses. Environ. Exp. Bot., 77, 283-287.

Schaller, J., Brackhage, C., Gessner, M. O., Bäuker, E., Gert Dudel, E., 2012a. Silicon supply modifies C: N: P stoichiometry and growth of *Phragmites australis*. Plant Biology, 14(2), 392-396.

Schaller, J., Faucherre, S., Joss, H., Obst, M., Goeckede, M., Planer-Friedrich, B., ... & Elberling, B., 2019. Silicon increases the phosphorus availability of Arctic soils. Sci. Rep., 9(1), 1-11.

Schaller, J., Hines, J., Brackhage, C., Bäucker, E., Gessner, M. O., 2014. Silica decouples fungal growth and litter decomposition without changing responses to climate warming and N enrichment. Ecology, 95(11), 3181-3189.

Schaller, J., Schoelynck, J., Struyf, E., Meire, P., 2016. Silicon affects nutrient content and ratios of wetland plants. Silicon, 8(4), 479-485.

Schaller, J., Struyf, E., 2013. Silicon controls microbial decay and nutrient release of grass litter during aquatic decomposition. Hydrobiologia, 709(1), 201-212.

Schmidt, M. W., Torn, M. S., Abiven, S., Dittmar, T., Guggenberger, G., Janssens, I. A., Kleber, M., Kögel-Knabner, I., Lehmann, J., Manning, D. A. C., Nannipieri, P., Rasse, D. P., Weiner, S., Trumbore, S. E., 2011. Persistence of soil organic matter as an ecosystem property. Nature, 478(7367), 49.

Schoelynck, J., Bal, K., Backx, H., Okruszko, T., Meire, P., Struyf, E., 2010. Silica uptake in aquatic and wetland macrophytes: a strategic choice between silica, lignin and cellulose? New Phytol., 186(2), 385-391.

Schoelynck, J., Struyf, E., 2016. Silicon in aquatic vegetation. Funct. Ecol., 30(8), 1323-1330.

Sivanesan, I., Park, S. W., 2014. The role of silicon in plant tissue culture. Front Plant Sci., 5, 571.

Soetaert, K., Hoffmann, M., Meire, P., Starink, M., van Oevelen, D., Van Regenmortel, S., Cox, T., 2004. Modeling growth and carbon allocation in two reed beds (*Phragmites australis*) in the Scheldt estuary. Aquat. Bot., 79(3), 211-234.

Song, A., Xue, G., Cui, P., Fan, F., Liu, H., Yin, C., Sun, W., Liang, Y., 2016. The role of silicon in enhancing resistance to bacterial blight of hydroponic-and soil-cultured rice. Sci. Rep., 6, 24640.

Song, Z., Liu, H., Zhao, F., Xu, C., 2014. Ecological stoichiometry of N: P: Si in China's grasslands. Plant Soil, 380(1-2), 165-179.

Street- Perrott, F. A., Barker, P. A., 2008. Biogenic silica: a neglected component of the coupled global continental biogeochemical cycles of carbon and silicon. Earth Surface Processes and Landforms: The Journal of the British Geomorphological Research Group, 33(9), 1436-1457.

Struyf, E., Conley, D. J., 2009. Silica: an essential nutrient in wetland biogeochemistry. Front Ecol. Environ., 7(2), 88-94.

Struyf, E., Conley, D. J., 2012. Emerging understanding of the ecosystem silica filter. Biogeochemistry, 107(1-3), 9-18.

Struyf, E., Mörth, C. M., Humborg, C., Conley, D. J., 2010. An enormous amorphous silica stock in boreal wetlands. J. Geophys. Res-Biogeo., 115, G04008.

Struyf, E., Van Damme, S., Gribsholt, B., Bal, K., Beauchard, O., Middelburg, J. J., Meire, P., 2007. *Phragmites australis* and silica cycling in tidal wetlands. Aquat. Bot., 87(2), 134-140.

Struyf, E., Van Damme, S., Gribsholt, B., Middelburg, J. J., Meire, P., 2005. Biogenic silica in tidal freshwater marsh sediments and vegetation (Schelde estuary, Belgium). Mar. Ecol. Prog. Ser., 303, 51-60.

Sun, T., Hobbie, S. E., Berg, B., Zhang, H., Wang, Q., Wang, Z., Hättenschwiler, S., 2018. Contrasting dynamics and trait controls in first-order root compared with leaf litter decomposition. P. Natl. Acad. Sci., 115(41), 10392-10397.

Suzuki, S., Ma, J. F., Yamamoto, N., Hattori, T., Sakamoto, M., Umezawa, T., 2012. Silicon deficiency promotes lignin accumulation in rice. Plant Biotechnol., 29(4), 391-394.

Talbot, J. M., Treseder, K. K., 2012. Interactions among lignin, cellulose, and nitrogen drive litter chemistry–decay relationships. Ecology, 93(2), 345-354.

Thevenot, M., Dignac, M. F., Rumpel, C., 2010. Fate of lignins in soils: a review. Soil Biol. Biochem., 42(8), 1200-1211.

664 Tubana, B. S., Babu, T., Datnoff, L. E., 2016. A review of silicon in soils and plants and its role in US
665 agriculture: history and future perspectives. Soil Sci., 181(9/10), 393-411.
666 Valkama, E., Lyytinen, S., Koricheva, J., 2008. The impact of reed management on wildlife: a meta-analytical
667 review of European studies. Biol. Conserv., 141(2), 364-374.
668 Vänskä, E., Vihelä, T., Peresin, M. S., Vartiainen, J., Hummel, M., Vuorinen, T., 2016. Residual lignin inhibits
669 thermal degradation of cellulosic fiber sheets. Cellulose, 23(1), 199-212.
670 Venterink, H. O., Güsewell, S., 2010. Competitive interactions between two meadow grasses under nitrogen
671 and phosphorus limitation. Funct. Ecol., 24(4), 877-886.
672 Wallace, A., Romney, E. M., Mueller, R. T., 1976. Nitrogen-silicon interaction in plants grown in desert soil
673 with nitrogen deficiency 1. Agron. J., 68(3), 529-530.
674 Wang, M., Gao, L., Dong, S., Sun, Y., Shen, Q., Guo, S., 2017. Role of silicon on plant–pathogen
675 interactions. Front Plant Sci., 8, 701.
676 Yamamoto, T., Nakamura, A., Iwai, H., Ishii, T., Ma, J. F., Yokoyama, R., Nishitani, K., Satoh, S., Furukawa, J.,
677 2012. Effect of silicon deficiency on secondary cell wall synthesis in rice leaf. J. Plant Res., 125(6),
678 771-779.
679 Yuan, J., Liu, D., Ji, Y., Xiang, J., Lin, Y., Wu, M., Ding, W., 2019. *Spartina alterniflora* invasion drastically
680 increases methane production potential by shifting methanogenesis from hydrogenotrophic to
681 methylotrophic pathway in a coastal marsh. J. Ecol., 107(5), 2436-2450.
682 Yue, K., Peng, C., Yang, W., Peng, Y., Zhang, C., Huang, C., Wu, F., 2016. Degradation of lignin and cellulose
683 during foliar litter decomposition in an alpine forest river. Ecosphere, 7(10), e01523.
684 Zang, J., Liu, S., Liu, Y., Ma, Y., Ran, X., 2016. Contribution of phytoliths to total biogenic silica volumes in
685 the tropical rivers of Malaysia and associated implications for the marine biogeochemical cycle. Chin. J.
686 Oceanol. Limn., 34(5), 1076-1084.
687 Zechmeister-Boltenstern, S., Keiblinger, K. M., Mooshammer, M., Peñuelas, J., Richter, A., Sardans, J., Wanek,
688 W., 2015. The application of ecological stoichiometry to plant–microbial–soil organic matter
689 transformations. Ecol. Monogr., 85(2), 133-155.
690 Zhai S. J., Xue L. L., 2016. Changes in the distribution of silica in the porewaters and sediments of the
691 intertidal zone with different plant communities in the Min River Estuary. Acta Ecologica Sinica, 36(21):
692 6766-6776.
693 Zhang, D., Hui, D., Luo, Y., Zhou, G., 2008. Rates of litter decomposition in terrestrial ecosystems: global
694 patterns and controlling factors. J. Plant Ecol., 1(2), 85-93.
695 Zhang, J., Zou, W., Li, Y., Feng, Y., Zhang, H., Wu, Z., Tu, Y., Wang, Y., Cai, X., Peng, L., 2015. Silica
696 distinctively affects cell wall features and lignocellulosic saccharification with large enhancement on
697 biomass production in rice. Plant Sci., 239, 84-91.
698 Zhu, S., Dai, G., Ma, T., Chen, L., Chen, D., Lü, X., Wang, X., Zhu, J., Zhang, Y., Bai, Y., Han, X., He, J., Feng,
699 X., 2019. Distribution of lignin phenols in comparison with plant-derived lipids in the alpine versus
700 temperate grassland soils. Plant Soil, 1-14.
701 Zukswert, J. M., Prescott, C. E., 2017. Relationships among leaf functional traits, litter traits, and mass loss
702 during early phases of leaf litter decomposition in 12 woody plant species. Oecologia, 185(2), 305-316.

703

Tables

Table 1 Concentrations and mass ratios between Si and other major nutrients in different tissues of *Phragmites australis*

	BSi (mmol g^{-1})	C (mmol g^{-1})	N (mmol g^{-1})	P (mmol g^{-1})	S (mmol g^{-1})	BSi/C	BSi/N	BSi/P	BSi/S
Stem	0.214 (0.096) *n*=67	38.378 (0.378) *n*=67	0.624 (0.171) *n*=67	0.018 (0.009) *n*=67	0.024 (0.009) *n*=67	0.006 (0.002) *n*=67	0.364 (0.185) *n*=67	14.789 (9.889) *n*=67	10.067 (6.577) *n*=67
Leaf	0.867 (0.309) *n*=67	36.343 (0.827) *n*=67	1.988 (0.228) *n*=67	0.056 (0.010) *n*=67	0.123 (0.031) *n*=67	0.024 (0.009) *n*=67	0.450 (0.198) *n*=67	16.380 (8.568) *n*=67	7.242 (2.642) *n*=67
Sheath	0.903 (0.427) *n*=65	35.885 (1.175) *n*=65	0.693 (0.086) *n*=65	0.023 (0.007) *n*=67	0.074 (0.021) *n*=66	0.025 (0.013) *n*=65	1.195 (0.704) *n*=65	46.430 (32.778) *n*=67	12.715 (5.703) *n*=66
Aboveground	0.478 (0.158) *n*=68	37.509 (0.451) *n*=68	0.943 (0.159) *n*=68	0.028 (0.009) *n*=68	0.055 (0.013) *n*=68	0.013 (0.004) *n*=68	0.519 (0.189) *n*=68	19.300 (10.069) *n*=68	9.062 (3.282) *n*=68

Note: the result is expressed by average values ± standard errors in mass ratio. The number in brackets is the standard error, and n represents the number of actual measured value.

Table 2 Regression models between BSi and C concentrations/storages in different tissues of *Phragmites australis*

The relationships of concentration per dry weight							
Item / Tissues	Y	X	Regression equation	N	R^2	*F* value	*P* value
Stem	BSi	C	—	67	—	—	—
Leaf			Y = -2.08X + 38.14	67	0.60	98.04	<0.001
Sheath			Y = -1.83X + 37.54	65	0.44	50.20	<0.001
Aboveground			Y = -1.48X + 38.21	68	0.27	24.01	<0.001
The relationships of storage per individual plant							
Item / Tissues	Y	X	Regression equation	N	R^2	*F* value	*P* value
Stem	BSi	C	Y = 260.50Ln(X) + 355.58	67	0.54	75.59	<0.001
Leaf			Y = 88.08Ln(X) + 81.14	67	0.38	40.62	<0.001
Sheath			Y = 41.65Ln(X) + 102.87	65	0.30	27.17	<0.001
Aboveground			Y = 450.77Ln(X) – 92.23	68	0.55	81.40	<0.001

Figures

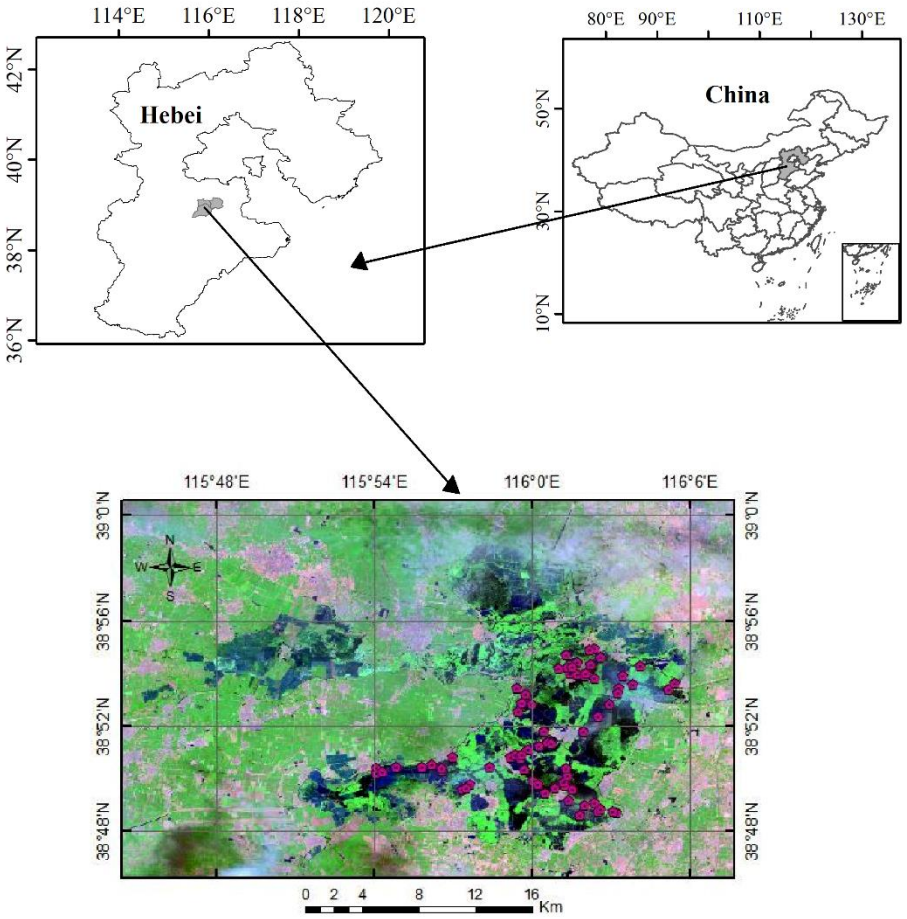

Fig. 1. Location of the regions in Baiyangdian wetland in Hebei province, China

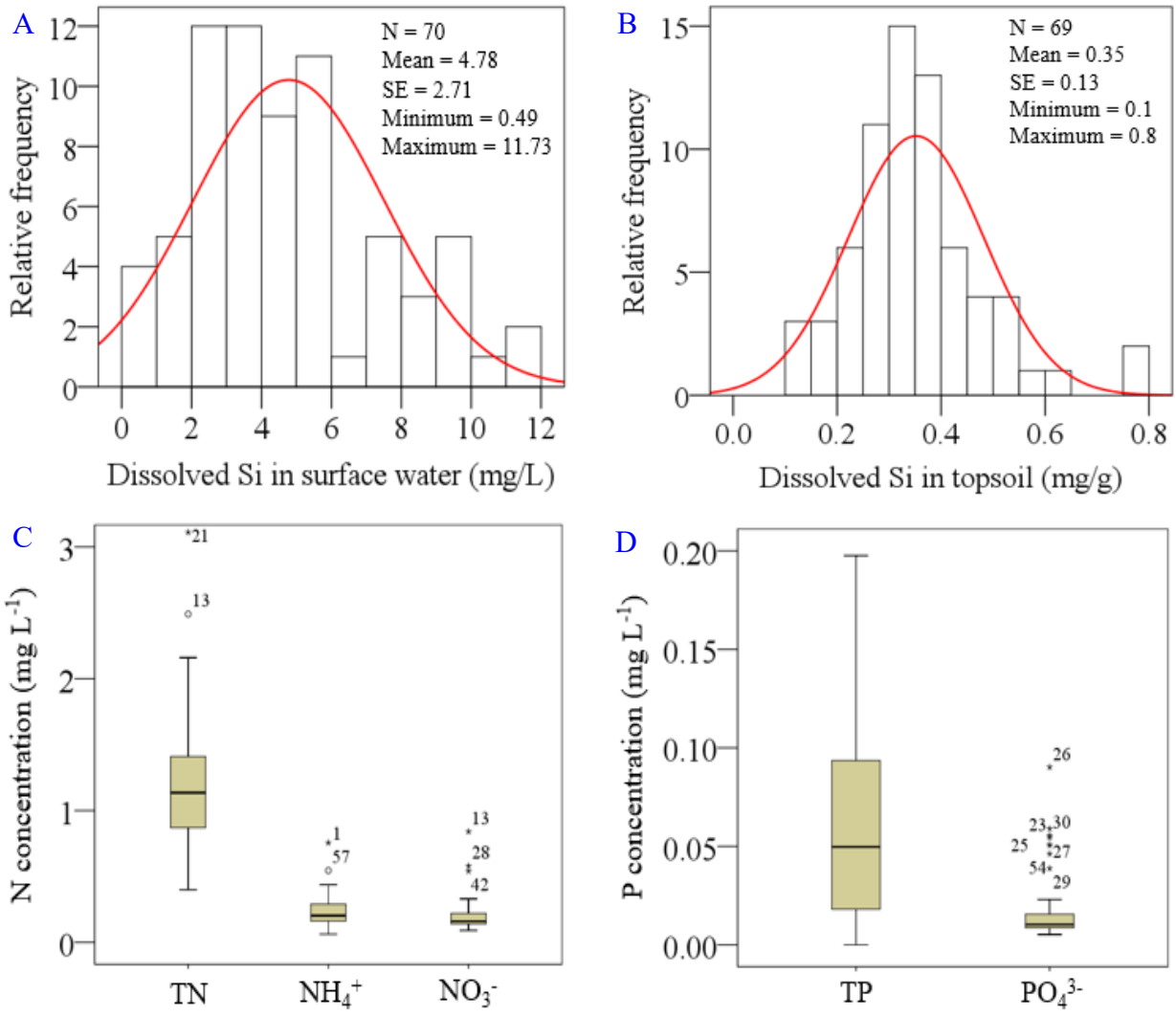

774 **Fig. 2.** The concentrations of dissolved Si in surface water (A), dissolved Si in topsoil (B), N (TN,

775 NH_4^+, NO_3^-) concentrations (C), and P (TP, PO_4^{3-}) concentrations in surface water (D).

776

777

778

779

780

781

782

783

784

785

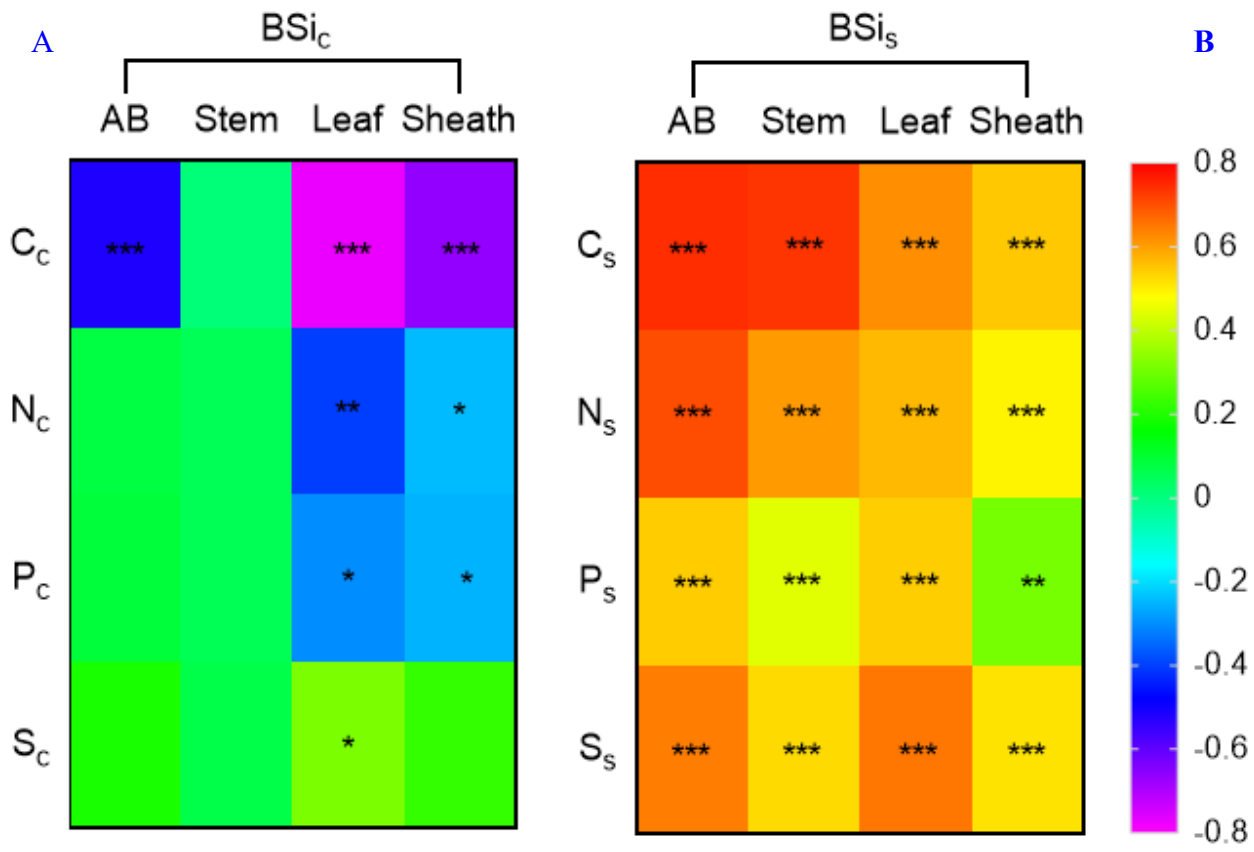

786 **Fig. 3.** Relationships between BSi concentration and C, N, P, S concentration in *Phragmites*
787 *australis* (A), relationships between total BSi uptake storage (biomass weight × content) and
788 aboveground biomass of C, N, P, S in *Phragmites australis* (B). AB, stem, leaf, and sheath
789 represent aboveground and different tissues of *Phragmites australis*, respectively. C_c, N_c, P_c, S_c,
790 and BSi_c represent the concentrations of C, N, P, S and BSi in plants, respectively. C_s, N_s, P_s, S_s,
791 and BSi_s represent the storage of C, N, P, S and BSi in plants, respectively.

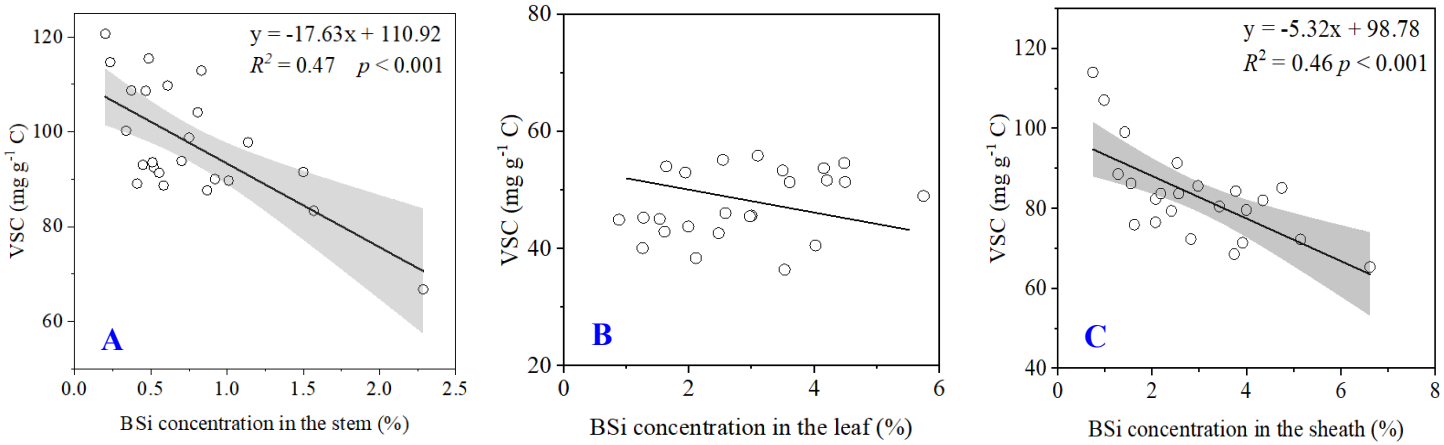

Fig. 4. Relationships between BSi concentrations and lignin (VSC phenols) concentrations in different tissues of stem (A), leaf (B) and sheath (C) of *Phragmites australis*. Dashed lines indicate 95% confidence interval.

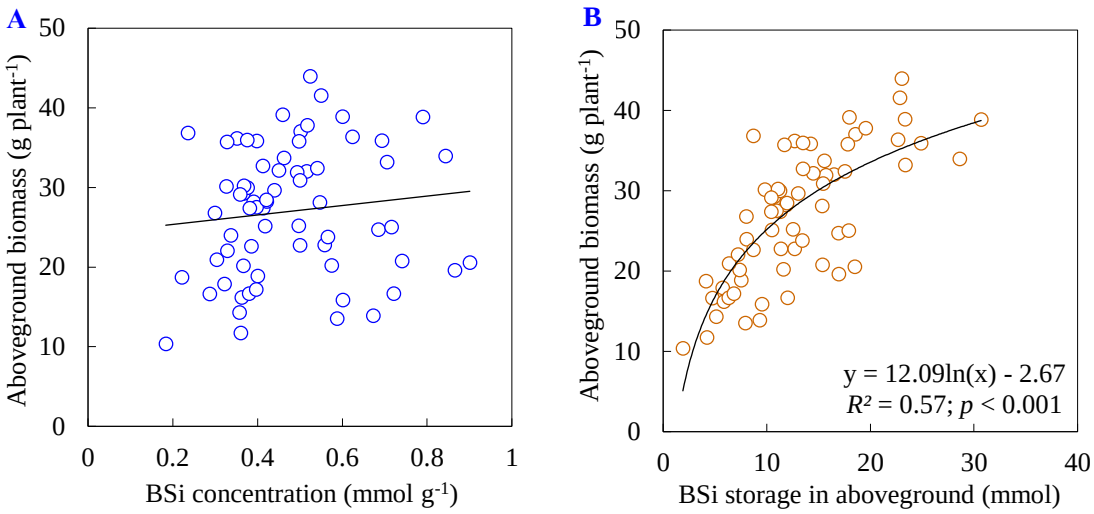

Fig. 5. Relationships between BSi concentration and total plant aboveground biomass of *Phragmites australis* (A), and BSi storage and BSi-mediated plant aboveground biomass of *Phragmites australis* (B).

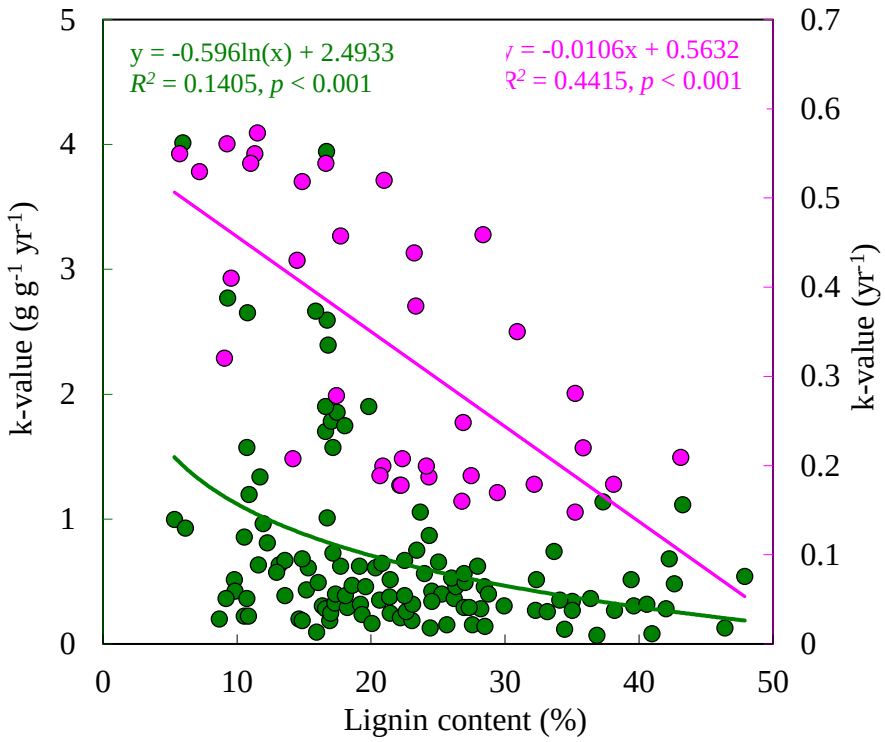

Fig. 6. Relationships between lignin content and litter decomposition rate constant (k). The left k (green color) was calculated using a first-order exponential decay function, the data are from 70 publishes studies at 110 sites; the right (pink color) was a function of the number of key traits measured in the 35 studied species, each symbol represents the average of one species (Zhang et al., 2008; Sun et al., 2018).

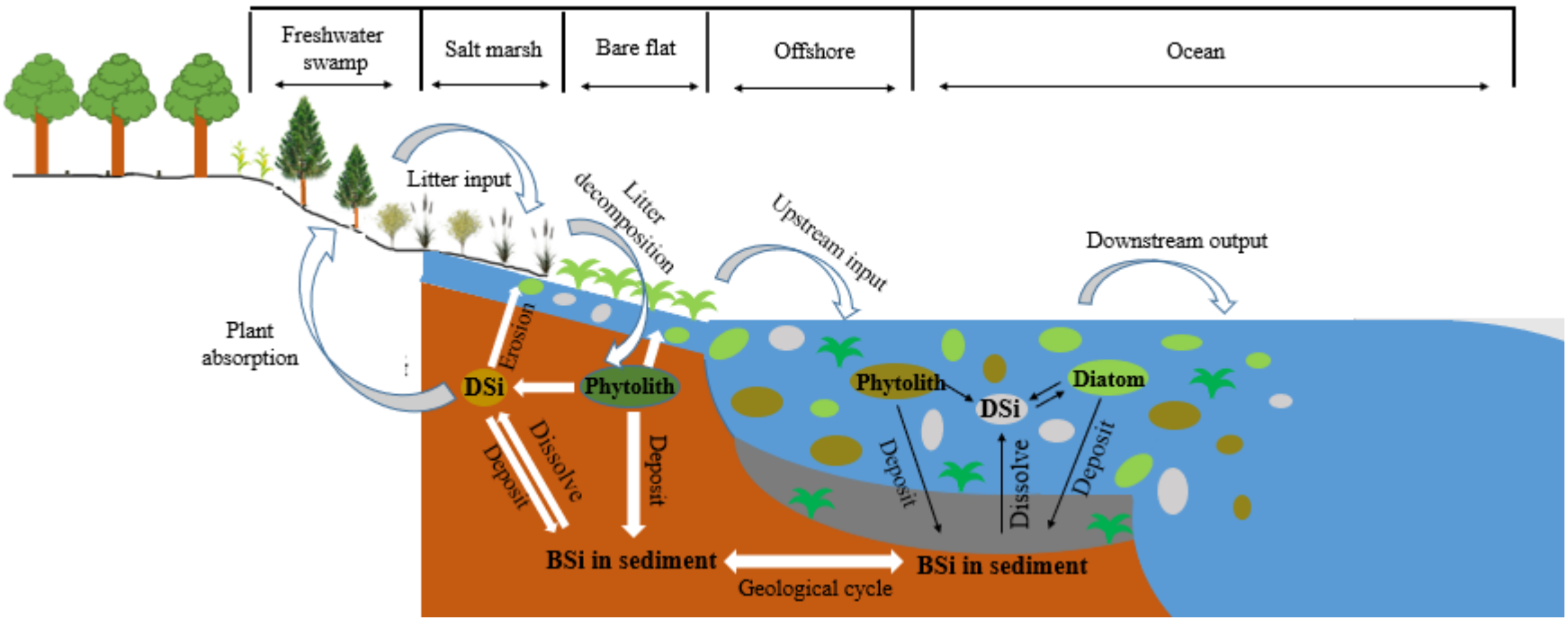

Fig. 7. Schematic showing the silicon-carbon coupled biogeochemical cycles along the land–ocean continuum